

## USES OF PULSED ELECTRON BEAM TO SOLID-STATES STUDIES

NORIAKI ITOH, TAKEYOSHI NAKAYAMA, KATSUMI TANIMURA,  
TAISU CHONG, MASAHIRO SAIDOH, KAZUMICHI NAKAGAWA  
and KAZUO SODA

*Department of Crystalline Materials Science, Faculty of Engineering*

(Received November 30, 1981)

### Abstract

A survey is given on the use of the pulsed electron beams to studies of solid states. Even though main emphasis is placed on the studies carried out at the Faculty of Engineering, Nagoya University, using the Pulsed Electron Facilities installed in 1970, the works carried out at other institutes are also included. Only the studies of crystalline solids with simple structures, such as alkali halides and aromatic hydrocarbons are covered. In the first place several instrumentations which have extended utilities of pulsed-electron beams are presented. Then we discuss the studies of the dynamics of excitons, emphasizing the advantages and disadvantages of the usage of the electron pulses. Then usages of the pulsed-electron beam for the studies of the excited states of the quasi-stable defects are described. Application of the electron pulse for studies of the excitation spectroscopy of the photochemistry is described. The dynamic studies of defects introduced by electron-pulse bombardment is discussed finally. A summary is given, which includes also the possible future experiments.

### CONTENTS

I. Introduction .....	165
II. Instrumentation .....	167
2. 1. Pulsed electron beam generator .....	167
2. 2. Modification of beam intensity .....	167
2. 3. Time-resolved optical spectroscopy .....	168
2. 4. Double excitation spectroscopy .....	170
2. 5. Dichroic breaching of unstable centers .....	171
2. 6. Measurements of volume expansion .....	173

III. Studies of the dynamics of excitons .....	174
IV. Studies of higher excited states of excitons .....	178
4. 1. Higher excited states of the self-trapped excitons in alkali halides .....	179
4. 2. Higher excited states of rare gas solids .....	181
4. 3. Higher excited states of triplet excitons in molecular crystals .....	182
V. Studies of the photochemical reaction and other non-radiative processes at highly excited states .....	184
5. 1. Kinetics of de-excitation and reactions at the excited states .....	184
5. 2. F-H-pair creation and intersystem crossing in NaCl and KCl .....	186
5. 3. Detrapping of impurity-trapped excitons by photo-excitation .....	188
VI. Dynamics of defects induced by ionizing irradiation in alkali halides .....	189
6. 1. Defect dynamics in the defect creation processes .....	189
6. 2. Dynamics of the primary defects .....	191
VII. Concluding remarks .....	193
References .....	193

## I. Introduction

Pulsed electron beams have been one of the most important experimental tools for development of the radiation chemistry and a number of facilities of the pulsed electron beams have been built for radiation chemists. A few reviews have been published in this field already.<sup>1)</sup> On the other hand the uses of the pulsed electron beam for studies of the radiation effects of solid states are not numerous. One of the intentions of this report is to point out that the pulsed electron beam is useful not only to studies of the radiation effects but also of the solid state properties themselves. We also intend to give a summary report on the way how the Febetron 707 installed at Nagoya University in 1970 have been utilized in these ten years. This pulsed electron beam generator has been used almost exclusively for solid state purpose.

It is known that energetic electrons with an energy of 1 MeV impose two types of effects on solids: (i) to produce electronic excitation and (ii) to impart kinetic energies on nuclei. The former is more frequent and the number of the electronic excitation can be calculated by dividing the absorbed energy (equal to the incident energy multiplied by number of incident electrons if the thickness is of the order of 1 mm) by so-called  $W$ -value, which is 2 ~ 3 times as large as the band-gap energy in most cases. The elastic collisions may cause the atomic displacements, resulting in the creation of the permanent defects. Number of defects created by an electron with an energy of 1 MeV<sup>2)</sup> is often of the order of  $10^{-3}$ . Thus we should realize that bombardments of a specimen with an electron pulse induce mostly electronic excitation. What we deal with in this paper is the effect of the electronic excitation and the effect of the elastic collisions is negligible in most cases.

The electronic excitation in solids creates electron-hole pairs and the excitons. In insulators, in which the binding energy of excitons is large, the electron-hole pairs are collapsed into the excitons. In some solids, in which the electron-lattice coupling is large, the excitons are self-trapped, as described in terms of the configuration coordinate diagram in Fig. 1.<sup>3)</sup> Upon the recombination of the free excitons or the self-trapped excitons, luminescence is often emitted. The configuration of the self-trapped exciton in alkali halides has been studied using

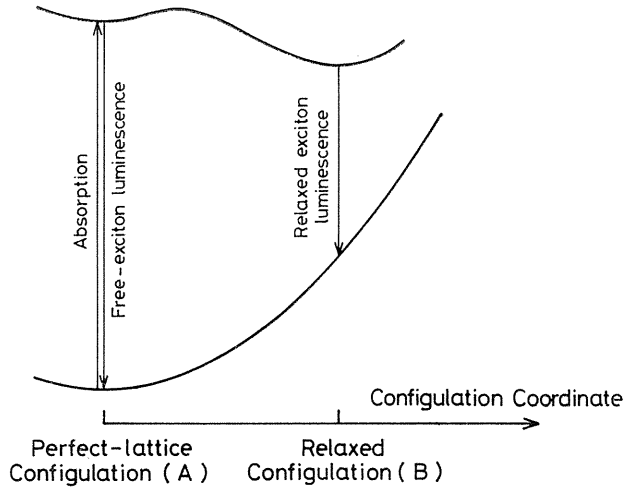


Fig. 1. The configurational coordinates curve indicating the optical absorption to create free excitons, the free-exciton luminescence and the relaxed exciton luminescence.

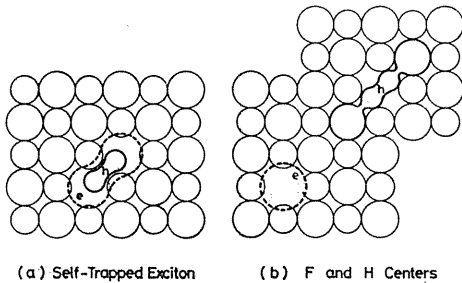


Fig. 2. The atomic configuration of the self-trapped excitons, the F centers and the H centers. The self-trapped exciton has approximately a configuration of a  $V_k$  center (self-trapped hole) plus an electron.

electron paramagnetic resonance and known to be an electron trapped by a self-trapped hole, a halogen molecular ion occupying two lattice points. It is also known that photochemical reactions cause defect creation at a certain excited state.<sup>4, 5)</sup> The atomic structure of the self-trapped exciton and of the photochemical products in alkali halides are depicted in Fig. 2.<sup>6)</sup>

In this paper we survey how the pulsed electron beams can be utilized for studies of these electronic excitation effects. We concentrate mainly to summarize the way of using the pulsed electron beams and its advantages and disadvantages. Even though the description is confined to the studies on alkali halides and aromatic hydrocarbon crystals, the studies can be easily extended to other solids. It is known that excitons in naphthalene have a character of the Frenkel excitons and are mobile.<sup>7)</sup> In alkali halides free excitons have a character of the Wannier excitons and have a relatively short life time (10 ps) until they are self-trapped.<sup>3)</sup> It is hoped that this survey could promote use of pulsed electron beams to other materials.

In this paper in II, we give instrumentation, which includes not only the

pulsed-electron source but also the attached instruments. We then proceed to the description of excitons (III), electronic structures of self-trapped excitons (IV), excitation spectroscopy of the photochemical processes (V) and finally the dynamics of the photochemical products (VI). In the summary we include the possible future applications.

## II Instrumentation

### 2. 1. Pulsed electron beam generator

There are two types of pulsed electron beam generators, which generate electron pulses capable of optical absorption spectroscopy: the linear accelerators (LINAC) and the Marx generators using low-impedance accelerating tubes. For the latter type, generators manufactured at the Field Emission Cooperation, called Febetron, are used most widely. Important specifications are that the accelerating voltage and current are about 10 MeV and 1 mA/cm<sup>2</sup> for LINAC, 2 MeV or 600 keV and 100 A/cm<sup>2</sup> for Febetron. The penetration depth of 10 MeV electrons are much larger than lower energy electrons. Therefore higher local concentration may be attained by low energy electrons but the total number of the effect of the electronic excitation, which is proportional to the absorbed power, is rather small for 600 keV Febetrons.

In Table 1 we show that pulsed electron beam generators used for solid state studies in this decades. In this table we omit facilities primarily aimed for the radiation chemical studies. The works having been carried out in the facilities shown in Table 1 will be discussed below.

Table 1. Pulsed electron beam generators used for solid state studies

location	type	substances studied
Nagoya Univ.	Febetron 707 (2 MeV)	Alkali halides Organic Crystals
Tohoku Univ.	Febetron 704 (600 keV)	Alkali halids
Tokyo Univ. (Institute of Solid State Phys.)	Febetron 704 (600 keV)	Rare gas solids
Naval Research Laboratory	Febetron 704 (600 keV)	Alkali halides Alkali earth fluorides
Tohoku Univ.	LINAC	Alkali halides
Tokyo Univ.	LINAC	Alkali halides
Argonne National Laboratory	LINAC	Alkali halides

### 2. 2. Modification of beam intensity

In using pulsed electron beams, it is often very important to change the beam intensity. This is not difficult for LINAC: by the modification of the injected

beam current. Because the Febetron is a constant impedance source, the change of the beam current requires to change the voltage, which induces the complication because of the change in the penetration depth.

In changing the beam intensity, we used two methods. To lower the intensity, we simply placed a copper plate with many small holes. The thickness of the copper plate was about 2 mm, which is larger than the electron penetration depth. Most serious problem in this method is the uniformity of the beam. It was confirmed, by using a microphotometer, that the uniformity over the width of 5 mm with a resolution of  $1\mu$  was obtained using  $1\text{ mm}\phi$  holes separated by 2 mm. Moreover, as described later, the intensity dependence of the luminescence decay of naphthalene was exactly the same as expected theoretically. These results give circumstantial support for the uniformity of the beam intensity.

In increasing the beam intensity, the magnetic field will be useful. We used a very simple method: We simply placed a tapered cylinder in front of the window of the accelerator tube. Apparently substantial fraction of the electrons emerging out of the window are guided by the tapered cylinder. The mechanism of focusing the beam is the build-up of the negative potential on the cylinder. This simple technique was used to increase the beam current density by a factor of five.

### 2.3. Time-resolved optical spectroscopy

The experimental apparatus used to obtain the change in the optical absorption spectrum induced by bombardment with an electron pulse is shown in Fig. 3. The specimen was placed in a light path of an optical system consisting of a Xe lamp, a monochromator and a photomultiplier. The change in the optical density of the specimen induced by bombardment with a pulsed electron beam causes the change in the output of the photomultiplier, which was detected using oscilloscopes. By changing the wavelength of the monochromator, the optical absorption spectra at a given delay time can be obtained.

A few precautions were taken to avoid the effect of the fluctuation of the intensity of the pulsed electron beams and the effect of radiation damage. As indicated in Fig. 3, we used always at least two detection systems, in one of which the wavelength of the monochromator was fixed and in the other the wavelength was scanned. This technique helped to obtain the shape of an optical absorption band accurately or the relative intensity of two

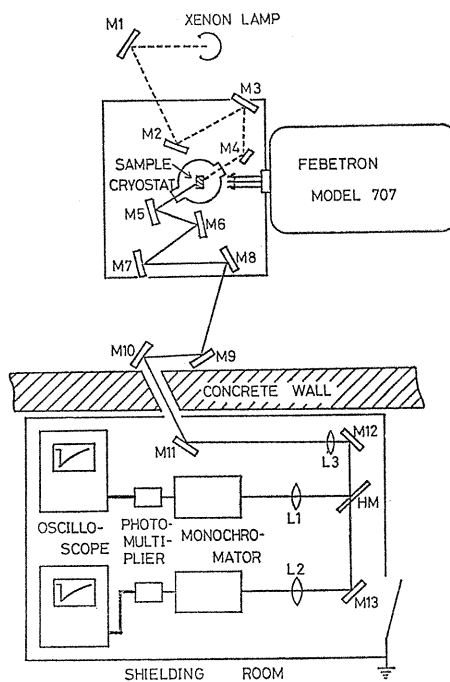


Fig. 3. The experimental arrangements for measuring the transient optical absorption change being used at Nagoya University. A long optical path and a good shielding facility are required to minimize the electromagnetic noise.

optical absorption bands. Sometimes when the effect of radiation was accumulated, it was necessary to anneal the specimen after bombardments. A typical oscilloscope trace of the optical absorption change is shown in Fig. 4 and a typical time-resolved spectra is shown in Fig. 5.

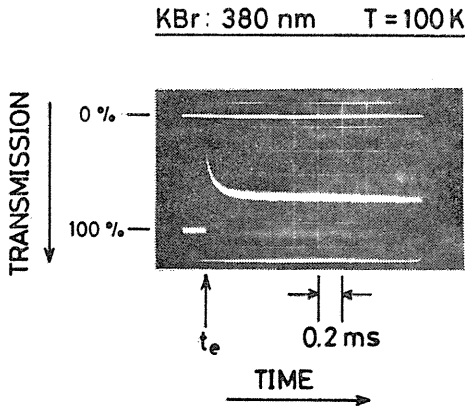


Fig. 4. A typical oscilloscope trace of the optical absorption change induced by an electron pulse at  $t_e$  from a Febetron generator. The time scale of the abscissa is 0.2 ms/div. The ordinate is a linear scale and the number shows transmission in per cent.

A more sophisticated method of obtaining time-resolved spectra of slowly changing species has been utilized by Williams.<sup>8)</sup> Their method is schematically shown in Fig. 6. In this technique they rotated a mirror using a turbine so that light output of the monochromator for various wavelength can be obtained in a time interval of the order of 100  $\mu$ s. Usage of a streak camera would facilitate the time-resolved optical absorption spectra in a much shorter time.

Time-resolved luminescence spectra can be obtained using a similar experimental equipment as that shown in Fig. 3, but without the light source. In some cases the luminescence disturbs the measurements of the optical absorption. If the luminescence is not too strong, the subtraction of the output voltage of the oscilloscope obtained without the light source from that with the light source suffices. When the luminescence intensity is very high, we often used a Xe flash lamp as a light source, which gives a

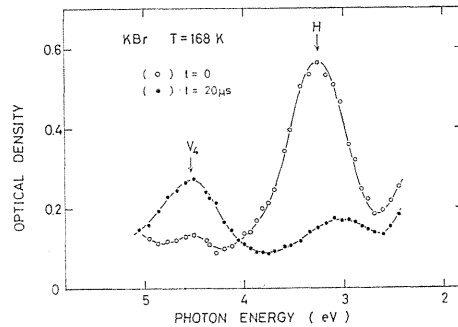


Fig. 5. Typical time-resolved optical absorption spectra obtained using the Febetron generator. The results indicate how the  $H$  centers (interstitial atoms) are annihilated and the  $V_4$  centers (the di- $H$  centers) are produced.

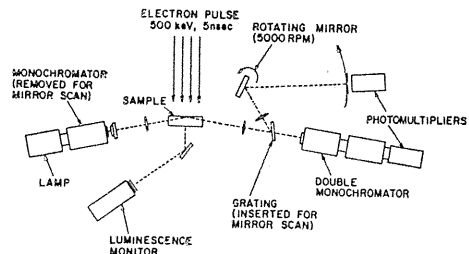
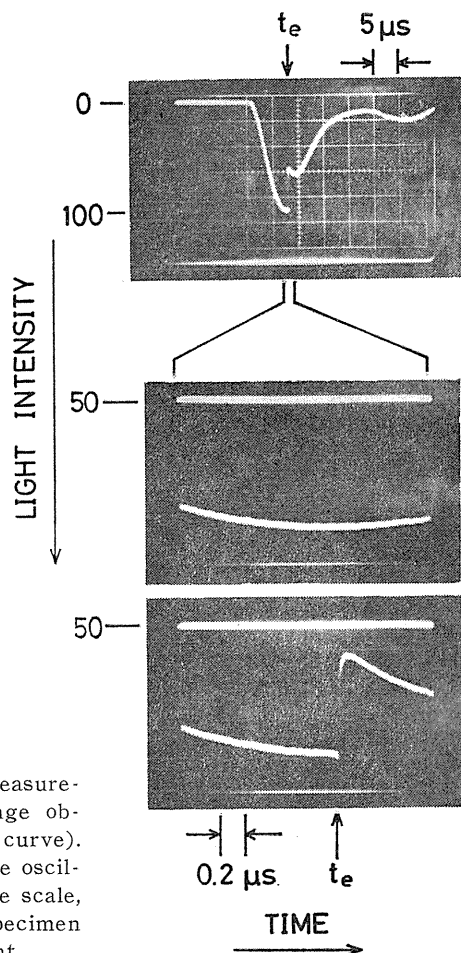


Fig. 6. Schematic diagram of the measurements of the optical absorption spectrum. A grating and a rotating mirror enable us to obtain optical absorption spectrum by a shot of an electron pulse (after Williams and Kabler<sup>8)</sup>).

microsecond light pulse triggered slightly before an electron pulse. The intensity of the Xe flash lamp is higher than the steady Xe lamp by a factor of 100. An example of the oscilloscope traces when a pulsed Xe lamp was used is shown in Fig. 7. Use of a laser, such as a He-Ne laser, helps when the wavelength scan is not necessary.

Measurements of the optical absorption spectra are known to provide us with information on the excited states of the localized states or of the color centers in solids. The time-resolved optical absorption spectroscopy yields information on the transient species. The transient species giving rise to transient optical absorption, more than  $1 \mu\text{s}$  after an electron pulse are quasi-stable defects or the radicals and lowest triplet state of the self-trapped excitons. We emphasize here that, because of the Jahn-Teller distortion, the lattice symmetry of the lowest state of the self-trapped exciton is generally lower than that of the perfect lattice. Thus the measurements of the optical absorption from the lowest self-trapped excitons yield information of the excited states of which the degeneracy is removed by the Jahn-Teller distortion. To measure the optical absorption change for an allowed transition, we need typically a concentration of the transient species of  $10^{16} \text{cm}^{-3}$ .

Fig. 7. A typical oscilloscope trace of the measurements of the optical absorption change obtained using a flash Xe-lamp (upper curve). The middle and lower figures show the oscilloscope traces of, in an extended time scale, the light transmitted through the specimen without and with electron bombardment.



#### 2. 4. Double excitation spectroscopy

The excitation spectra for luminescence of color centers in ionic crystals have been measured extensively and found to be useful to derive information on the lattice relaxation. Similarly we may expect that measurements of the luminescence induced by the excitation of a transient species, such as the self-trapped exciton may yield information on the relaxation from highly excited states of the self-trapped excitons. For example, the excitation spectrum of the creation of the singlet luminescence by the photo-excitation of the lowest triplet exciton may yield information on the mechanism of the intersystem crossing. This intersystem crossing from the triplet manifold to the singlet manifold has been measured using ex-

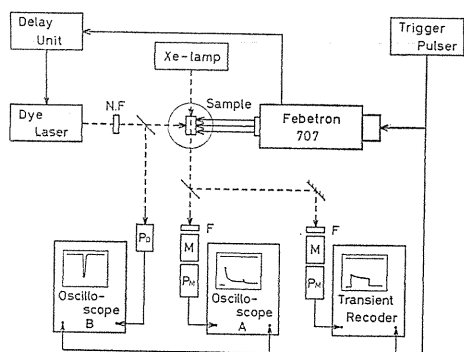


Fig. 8. Schematic diagram of the experimental apparatus for double excitation spectroscopy, utilizing excitation with an electron pulse and a laser pulse. The laser pulse is delayed from the electron pulse using the delay unit. The Xe lamp is used only for the absorption measurements. Xe lamp light through the specimen or light emitted from the specimen are guided into a few optical detection systems so that a few pieces of information are derived from a single shot.

perimental apparatus shown in Fig. 8. Here the triplet excitons are generated using an electron pulse and then they are excited to higher states using a dye laser. The induced singlet luminescence and the decrease of the triplet luminescence at the incidence of the light pulse were measured. Comparison of these two quantities yields fractional yield of the intersystem crossing, and the dependence of the fractional yield on the photon energy gives information on the non-radiative processes.

It is also known that excitation of color centers often causes photochemical changes. The excitation spectroscopy of these photochemical changes is often very important to understand the mechanism. One of the photochemical processes which has attracted scientists for these decades is the creation of a Frenkel pair of an F center (a vacancy) and an H center (an interstitial) from an exciton in alkali halides. An excitation spectroscopic study could be made using ultra-violet light which create excitons from the ground state. An alternative approach is the double excitation, namely to excite the self-trapped exciton. This double excitation technique is similar to the double excitation study of the intersystem crossing. Only the difference is that we measure the optical absorption due to the F centers or the H centers instead of the singlet luminescence, using a Xe-lamp as shown in Fig. 8. Similarly to the intersystem crossing, the measurement of the dependence of the yield on the photon energy of the laser light is useful for the purpose of understanding the mechanisms of the photochemical processes. We emphasize again that the double excitation spectroscopy for both the photochemical reaction and the intersystem crossing can survey the excited states at the relaxed configuration (configuration B in Fig. 1), while the excitation spectroscopy (single excitation spectroscopy) from the ground state can survey the excited states at the configuration of the perfect lattice (configuration A in Fig. 1). Thus the information derived from the double excitation spectroscopy is much more penetrating than the single excitation spectroscopy.

It is to be noted that both the intersystem crossing and the photochemical reaction remove the self-trapped exciton from the triplet manifold. In the other words the triplet self-trapped excitons are bleached by irradiation with laser light. We can use this fact for measuring the dichroic bleaching, as described in the next section.

### 2. 5. Dichroic bleaching of unstable centers

The optical absorption spectroscopy of a color center can locate the excited



states and in some cases the measurements of the shape of the optical absorption band yield the information on the electron-phonon coupling at the excited states. The direction of the optical transition dipole moment from the ground state to a higher state of a center with a low symmetry, may be determined by the dichroic bleaching experiments, in which the specimens are bombarded with light polarized along a certain crystalline direction to cause bleaching of the color centers being studied and subsequently optical absorption of the specimens is measured with light polarized along the directions parallel and perpendicular to the bleaching light. The dichroic bleaching experiments being dealt with in this section is very similar to the techniques described above except that the initial state of the optical absorption is the ground state of an unstable center. This technique can be used to study the optical transition from the lowest excited states of a center to a higher state. The schematic diagram of the experimental apparatus for the dichroic bleaching experiment is shown in Fig. 9. Here a specimen is bombarded first by a pulsed electron beam to create excited states. Then the specimen is left for a  $1\ \mu\text{s} \sim 1\ \text{ms}$ , during which the several short-lived excited states are allowed to be de-excited, leaving only rather stable transient centers. Then the specimen

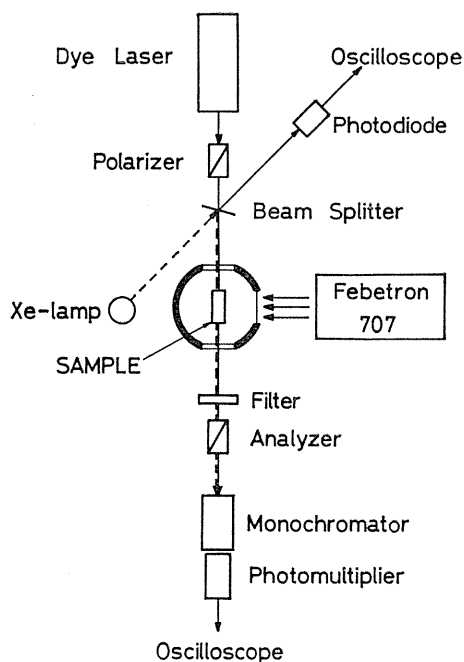


Fig. 9. Schematic diagram for dichroic bleaching experiments of an unstable species generated by bombardment with an electron pulse. A polarizer picks up light polarized along a certain direction, while the analyzer is used to determine the degree the polarization of light from the Xe-lamp transmitted through the specimen or luminescence from the specimen.

is bombarded with a light pulse from a tunable dye laser polarized along a certain direction. Then we measure the luminescence or the optical absorption change, induced by the irradiation with a light pulse, through a polarizer oriented parallel or perpendicular to the bleaching light.

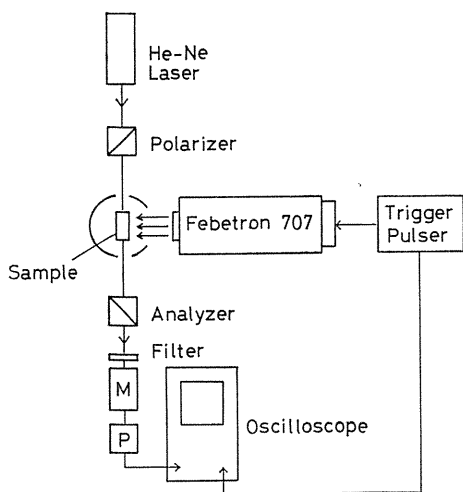
In order to make such measurements, the substantial fraction of the lowest excited states should be excited. Suppose  $\sigma$  be the cross section for the optical

excitation and  $\phi$  be the number of photons per  $\text{cm}^2$  in a light pulse,  $\sigma\phi$  is the probability for the center to be ionized. Thus we need  $\sigma\phi \sim 1$ . In most experiments we have used a flush-lamp-pumped dye-laser, which generate light pulses of 1 mJ in the wavelength range between  $4000\text{\AA}$  and  $7000\text{\AA}$ .

The technique has been first developed by Williams to obtain the transition dipole moment from the lowest state of the self-trapped excitons in alkali halide to higher states. He used a Ruby laser as a light source of dichroic bleaching. We shall see later that much more information can be derived by measuring the excitation spectrum for the dichroic bleaching.

### 2.6. Measurements of volume expansion

The optical absorption spectroscopy and luminescence spectrum yield information on the local nature of defects created by the electron irradiation. Sometimes it is important to compare the results of optical measurements with macroscopic properties of the specimen. One of the most important macroscopic properties of solids relevant to the studies of radiation effect is the volume expansion. If defects are created, the lattice volume expands in proportion to the number of defects. The measurements of the volume expansion due to the irradiation and of



M: Monochromator  
P: Photomultiplier

Fig. 10. Schematic diagram of the experimental apparatus for measurement of the volume expansion induced by irradiation with an electron pulse. A sample is placed between a polarizer and an analyzer, and irradiated partially with an electron pulse. The stress caused by the expansion of the irradiated part gives rise to light transmission through the system.

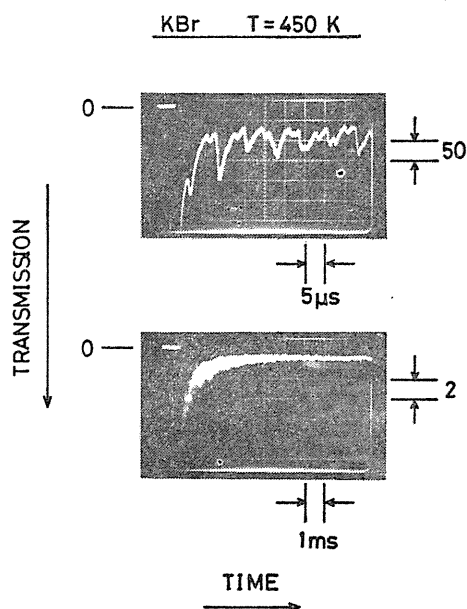


Fig. 11. A typical oscilloscope trace of the measurements of lattice expansion induced by an electron pulse on KBr. The apparent oscillation is due to the sound wave reflected back and forth in the specimen.

its annealing can decide whether defects are indeed created or annihilated or defects are simply rearranged. More specifically if the Frenkel defects, pairs of a vacancy and an interstitial, are annihilated, the volume change takes place, while either of vacancies and interstitials changes their form, no change in volume expansion takes place even though the optical properties are modified. An advantage of measuring the volume expansion induced by a pulsed electron beam is that one can pursue the behaviors of defects at a high concentration in a microsecond time scale.

Most conventional technique of measuring the volume expansion that has a short response time is the photoelastic technique. In this technique a specimen is placed in an optical path between two crossed polarizers. In the absence of the distortion in the specimen no light passes through the system. When a part of the specimen is irradiated, the distortion arises near the boundary, causing the so-called optical rotation. Then the system becomes partially transparent, the light output being proportional to the degree of the optical rotation and hence the volume expansion of the irradiated part.

The photoelastic technique has been applied to the studies of radiation damages of insulating solids since 1950's, only for the continuous irradiation.<sup>9)</sup> We have used the technique to study the transient response of specimens induced by an electron pulse. The block diagram of the experimental apparatus is shown in Fig. 10. A typical oscilloscope trace of the output of the photomultiplier is shown in Fig. 11. The decaying oscillation is due to the elastic wave travelling back and forth in the specimen. When the oscillation is averaged, one obtains the volume expansion of the specimen. In the figure a result of the measurements at high temperatures is shown, where substantial part of defects are annealed in a millisecond range.

### III. Studies of the dynamics of excitons

Excitons are important entity for the energy transport in crystalline solids. Their dynamic properties, such as diffusion constants and reaction rate constants with impurities or defects, attracted interest of many scientists. Reaction among excitons taking place at a high density, namely the high-density effects, are problems of current interest.<sup>10, 11)</sup>

The pulse technique is useful for studies of the exciton dynamics. The excitons may be introduced in a specimen by either a light pulse or an electron pulse and the luminescence emitted upon the recombination of excitons or that induced by the exciton-impurity interaction is measured. Light pulses have been used extensively. Advantages of using electron pulses are as follows: (1) Because of high intensity, the luminescences over a wide range of exciton concentration can be measured. (2) Because of the large penetration depth of electrons the exciton concentration in the specimen can be regarded as uniform. (3) Singlet and triplet excitons can be easily generated in crystals having a wide band gap. The disadvantage is the possible introduction of lattice defects by the radiation damages. This disadvantage can be avoided by carrying out measurements under a condition that the exciton concentration and the impurity concentration with which the exciton interaction is being studied exceeds the concentration of the radiation-induced

defects.

We describe first the studies of the exciton interaction in a naphthalene crystal. In these crystals, several types of exciton interactions, between singlet excitons S, between triplet excitons T, and between singlet and triplet excitons have been invoked.<sup>10)</sup>



where G denotes the ground state. Figure 12 shows the time change of the luminescence from the singlet excitons introduced by an electron pulse of several intensities.<sup>12, 13)</sup> The strong dependence of the characteristics of the decay curves on the intensity of the electron pulse evidences the exciton-exciton interaction particularly the singlet-triplet exciton interaction.\* The annihilation of excitons can be described in terms of kinetic equations involving the exciton interaction described. The solutions of the kinetic equations are shown by solid lines in the figure. The good agreement over a large dynamic range assures the technique is promising. The decay curve of luminescence for small  $t$  is governed mainly by the interaction (2) and for large  $t$  is by the interaction (3). In the latter region the decay kinetics is a bimolecular reaction: the intensity  $I$  of the singlet luminescence follows the relation

$$\left(\frac{I_0}{I}\right)^{1/2} - 1 = kt, \quad (4)$$

where  $t$  is time,  $I_0$  is the luminescence intensity at  $t=0$  and  $k$  is the reaction rate constant between two triplet excitons and is given by

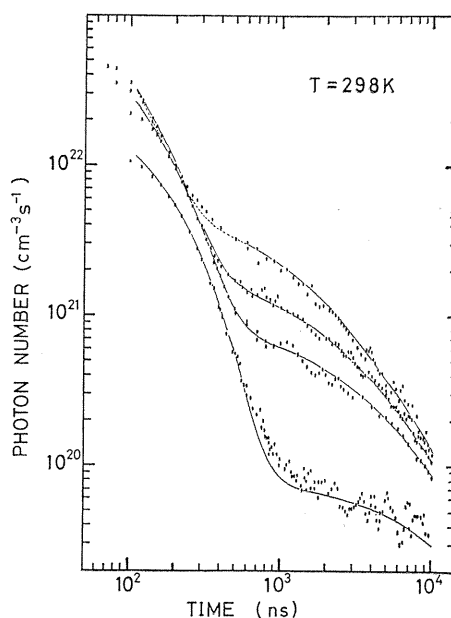


Fig. 12. Decay of luminescence in a naphthalene crystal at 298K induced by an electron pulse of several intensities. The intensity ratio is 1 : 3.5 : 7.1 : 12. Note that there are crosses in the decay curves (see text). (after Fujiwara et al.<sup>13)</sup>)

\* Without the singlet-triplet exciton interaction, the concentration of the singlet excitons should follow the same annihilation curve irrespective of the intensity of the electron pulse, thus the time dependence of the luminescence intensity will never cross. With the singlet-triplet exciton interaction, the crossing will take place because the different rate constants of reactions (1) and (2) causes the difference in the concentration of singlet and triplet excitons immediately after the electron pulse.

$$k = 4\pi DR, \quad (5)$$

where  $D$  is twice the diffusion constants (since two excitons are moving) and  $R$  is the interaction radius.

The effect of the radiation damage on the luminescence of naphthalene has been observed after the concentration of the singlet excitons becomes low, where the singlet excitons are generated by collisions of two triplet excitons.<sup>14)</sup> Typical experimental result of the radiation effect on the singlet luminescence decay is shown in Fig. 13. The open circles show results obtained with the first electron pulse on a virgin specimen. Clearly it follows Eq (4). The results after several shots of electron pulses are also shown in the figure. Obviously the decay rate becomes faster with increasing the number of shots. Such experimental results have enabled us to obtain the rate constant between the excitons and the radiation-induced defects.

The reaction rate constant can be also determined through measurements of the build-up of the luminescence from impurities that are activated through interaction with excitons. It is more confirmative if one measures both the annihilation of excitons and build-up of the impurity luminescence at the same time. Such a study has been carried out for NaCl:Li,<sup>15)</sup> the results of which are shown in Fig. 14. In NaCl:Li, both the exciton luminescence and impurity luminescence

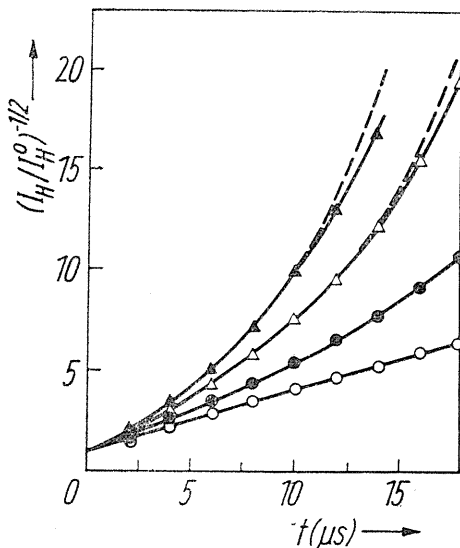


Fig. 13. The dependence on time  $t$  of the fluorescence intensity  $I_H$  divided by that at  $t=0$  in a naphthalene crystal at 20K undamaged (open circles) and damaged by electron pulses. The closed circles, open triangles and closed triangles are obtained after 10, 20 and 40 shots. (after Chong and Itoh<sup>14)</sup>)

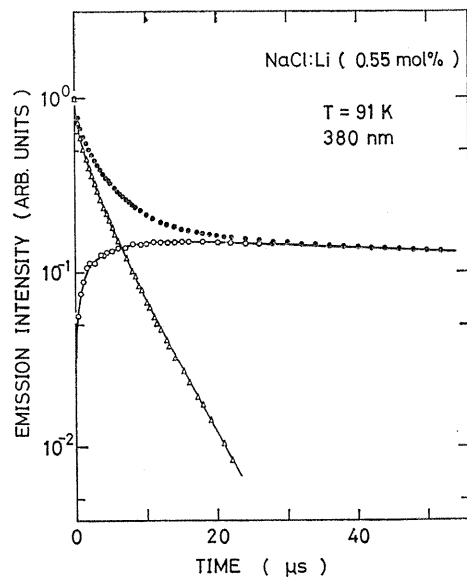


Fig. 14. Decomposition of the observed luminescence intensity in NaCl:Li into the component of unperturbed self-trapped exciton (open triangles) and self-trapped exciton perturbed by  $\text{Li}^+$  (open circles). (after Tanimura and Itoh<sup>15)</sup>)

exhibit broad bands overlapping each other. The closed circles in the figure denote the decay of the cumulative luminescence. Using the difference in the peak positions and widths of the exciton luminescence band and of the impurity luminescence band and the results of measurements of the luminescence decays at several wavelengths, the cumulative luminescence decay was decomposed into the decay of the exciton luminescence and the build-up of the impurity luminescence, as indicated by open triangles and open circles, respectively, in Fig. 14. Curvature observed in the decay curve of the exciton luminescence has been shown to be indicative of the diffusion-limited reaction between close exciton-impurity pair. If this effect is included the reaction rate constant is given by<sup>16)</sup>

$$k = 4\pi DR \left( 1 + \frac{R}{\sqrt{\pi Dt}} \right), \quad (6)$$

where  $t$  is time elapsed after excitons are distributed uniformly in solids.

So far we have discussed the diffusion-limited reaction between two excitons and between an exciton and an impurity. In alkali halides doped with silver or thallium ions, which are efficient electron traps, the electrons are trapped by the impurities to form  $\text{Ag}^\ominus$  or  $\text{Tl}^\ominus$  and holes are self-trapped. In such a case most of electrons and holes created remain almost permanently after irradiation at the temperatures where the self-trapped holes are stable. However, some of the pairs that are generated in proximity recombine in a short time through the tunneling process. This tunneling recombination exhibits luminescence that decays very slowly. Since the pulsed electron beam can generate the tunneling pairs at a high concentration, it is possible to measure the luminescence decay over a long dynamic range. A typical example of the tunneling luminescence in  $\text{NaCl}:\text{Ag}$  and  $\text{KCl}:\text{Ag}$  is shown in Fig. 15.<sup>17)</sup> The results indicate that the intensity  $I$  of the luminescence decays following a relation

$$I = I_0 \left( \frac{t_0}{t} \right)^n, \quad (7)$$

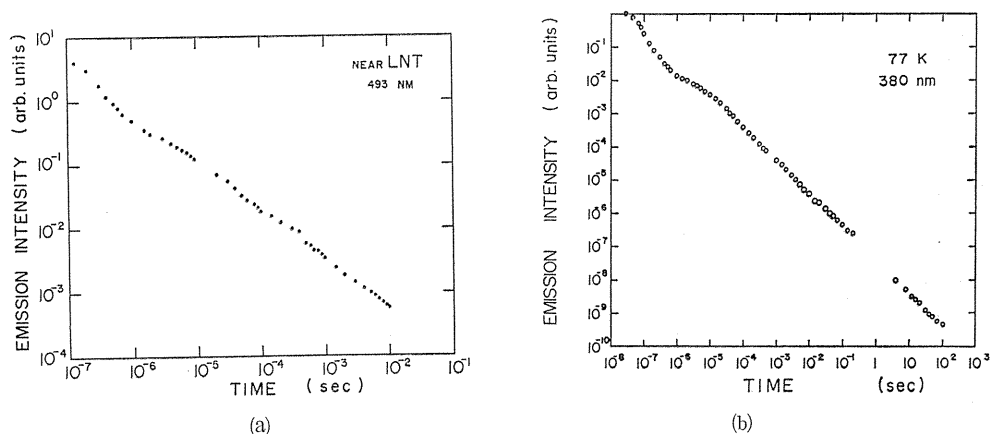


Fig. 15. Decay curves of the tunneling luminescence between neutral silver centers and  $V_k$  centers formed by bombardment with an electron pulse in  $\text{KCl}$  (a) and  $\text{NaCl}$  (b). (after Tashiro et al.<sup>17)</sup>)

where  $t$  is time,  $I_0$  is the intensity at  $t=t_0$ , immediately after an electron pulse and  $n$  is the index. It is found that  $n$  is unity in NaCl but 0.77 in KCl. The difference has been attributed to the difference in the anisotropic nature in the tunneling recombination. If all pairs recombine by nearly the same rate irrespective of the direction of the vector adjoining the pair,  $n$  expected to be about 0.8. If only pairs oriented along a certain crystalline direction give rise to the tunneling luminescence,  $n$  is expected to be unity.

Studies described above can be extended to various types of insulating materials, inorganic and organic crystals and polymers. We emphasize that the advantage of using an electron pulse to create excitons is that it creates excitons uniformly over a large volume at a concentration of up to  $10^{19}\text{cm}^{-3}$ . Thus the decay can be studied over a large dynamic range even before the concentration of excitons becomes lower than impurity concentration in the specimen.

#### IV. Studies of higher excited states of excitons

The color centers in alkali halides are subjects that have attracted interest of scientists over half a century.<sup>18, 19)</sup> Through the studies of the color centers, the methods of clarifying the electronic structures of defect states have been well established. Among them, here we note mainly the optical techniques. The optical absorption and luminescence spectroscopies are standard techniques. The dichroic bleaching experiments, in which color centers are bleached with light polarized along a certain crystalline direction to populate the specimen with color centers oriented along a given crystalline direction, are often useful to determine the direction of the optical transition dipole of color centers with low symmetry. The studies of the correlation of polarization of exciting light and emitted light of a luminescence center yield similar information. Measurements of the excitation spectrum for luminescence and a certain photochemical reaction has been found useful to make clear the energy transfer process.

The conventional technique described above has been extensively used for studies of stable defects or color centers. In nature there are many color centers that are not stable even at the lowest temperature but yet studies of their electronic states are of fundamental importance. The pulsed electron beam is useful to study the electronic structures of the transient color centers, because an electron pulse can create transient color centers by an amount sufficient to use the optical spectroscopic techniques described above. Self-trapped excitons can be regarded as a type of the transient color centers. On the other hand, the optical absorption from free excitons have characters different from the localized centers. Here we describe typical experimental achievements of the optical studies of the self-trapped excitons in alkali halides and of free excitons of naphthalene. The self-trapped excitons in alkali halides are not only the typical self-trapped states in solids but also known to be the origin of the photochemical process: a Frenkel pair (a pair of a vacancy and an interstitial) is created from a self-trapped exciton. The atomic structure of the self-trapped exciton is known through EPR works and shown in Fig. 1, and its one-electron energy diagram is shown in Fig. 16.

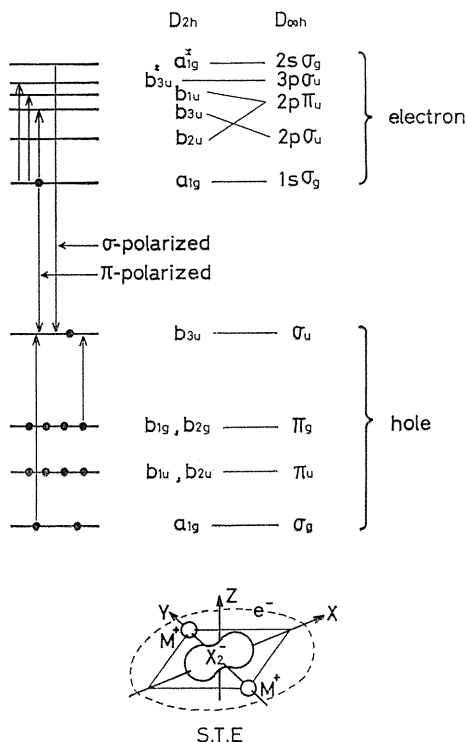


Fig. 16. One-electron orbitals of the self-trapped excitons in alkali halides. Energy intervals are those at the configuration of the lowest triplet state in KCl. The occupation at the lowest state is indicated.

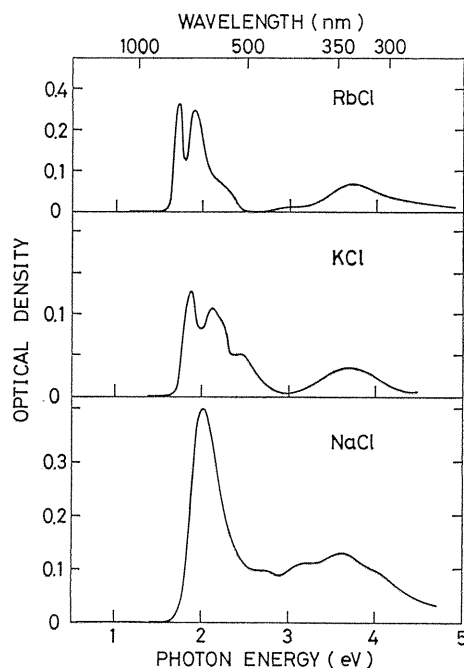


Fig. 17. Optical absorption spectra of self-trapped exciton in alkali chlorides (after Kabler and Williams<sup>8)</sup>)

#### 4. 1. Higher excited states of the self-trapped excitons in alkali halides

Using the experimental technique described in 2. 3, measurements of the optical absorption spectrum of the lowest state of the triplet self-trapped excitons have been made by Williams and Kabler.<sup>8)</sup> Typical results are shown in Fig. 17. They pointed out that the optical absorption bands at the lower energy side is due to the transition of the electron of the self-trapped exciton, based on mainly the results that their peak position depends on the lattice constant in a similar way to electron-trapped centers in alkali halides. On the other hand the optical absorption band at the higher energies have been ascribed to the transitions in  $\text{Cl}_2^-$ -molecular ion or the hole transition (note that a self-trapped exciton is an electron trapped by a self-trapped hole ( $\text{Cl}_2^-$ -molecular ion)). Further detailed assignment of the transitions can be made by employing the dichroic bleaching experiments.

The dichroic bleaching experiment of the self-trapped excitons has been first carried out by Williams,<sup>20)</sup> but in more complete form by Soda et al.<sup>21)</sup> The experimental technique used by the latter authors has been described in 2. 5. A specimen populated with self-trapped excitons was further bombarded with a light pulse polarized along a  $\langle 110 \rangle$  direction and the laser-light-induced change in the



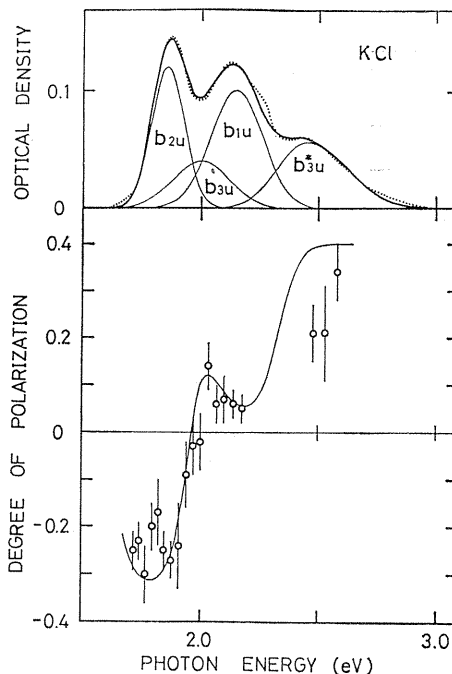


Fig. 18. Decomposition of the optical absorption band of the self-trapped exciton into components. In the lower half the degree of polarization as a function of photon energy is shown. The solid line in the lower half is the calculated curve based on the decomposed components shown in the upper half. (after Soda *et al.*<sup>21)</sup>)

$\pi$ -luminescence was measured through a polarizer either oriented along parallel or perpendicular to the direction of polarization of the bleaching light. From the degree of polarization of the luminescence change, one can determine the direction of the optical transition dipole moment as a function of photon energy. The results for KCl is shown in Fig. 18. It turns out that the degree of polarization depends on the photon energy of the laser light, indicating that the optical absorption bands, such as shown in Fig. 17, are composites. Since the electron in the lowest self-trapped exciton is in the  $1s(a_{1g})$  orbital, the transition to the  $p$ -type orbitals is allowed. In  $D_{2h}$  symmetry, the  $2p$ -orbitals are split into three sublevels, a  $\sigma$ -polarized and two  $\pi$ -polarized sublevels as indicated in Fig. 16. The optical transition to the orbitals higher than  $2p$  may not be able to be separated. Thus it was assumed that the optical absorption band associated with the electron transition shown in Fig. 17 consists of four absorption bands, three bands for  $1s$ - $2p$  transitions and a band for the mixtures of transitions to the higher states. Then they obtained the peak position and the half-width of each absorption band as fitting parameters, so that the calculated optical absorption spectra (thick solid line in the upper half of Fig. 18) and the calculated wavelength dependence of the degree of polarization (solid line in the lower half of Fig. 18) agree with the experimental data (dotted line in the upper half and open circles in the lower half of Fig. 18).

The transition energy to the higher excited states of the self-trapped excitons is summarized in Table 2. We note that these transition energies are those at the relaxed configuration. At the unrelaxed configuration, the  $2p$ -orbitals are degenerate. Upon relaxation, the exciton may be relaxed into one of these higher excited

Table 2. The optical absorption of the self-trapped excitons in alkali chlorides. The numbers in the parenthesis of the transition energies are those for the  $F_2$  centers. (After Soda et al.<sup>2u</sup>)

Material	Assignment	Experimental			Theoretical transition energy (eV)		
		Transition energy (eV)	FWHM (eV)	Relative oscillator strength	CNDO	Pseudo-potential	Hartree-Fock
NaCl	$a_{1g} \rightarrow b_{2u}$	2.00	0.26	1.0		2.3~2.4 <sup>a)</sup>	1.49 <sup>b)</sup>
	$a_{1g} \rightarrow b_{3u}$	2.02	0.30	0.35		0.7~1.1	
	$a_{1g} \rightarrow b_{1u}$	2.25	0.33	0.83		2.3~2.4	
	$a_{1g} \rightarrow b_{3u}^*$	2.65	0.40	0.64		2.3~2.5	
			0.75				
KCl	$a_{1g} \rightarrow b_{2u}$	1.86(2.27) <sup>d)</sup>	0.16	1.0	1.9±0.15 <sup>c)</sup>	2.1~2.2 <sup>a)</sup>	
	$a_{1g} \rightarrow b_{3u}$	2.00(1.54)	0.28	0.58	1.36	0.70	
	$a_{1g} \rightarrow b_{1u}$	2.15(1.30)	0.26	1.4	2.2±0.15	2.1~2.2	
	$a_{1g} \rightarrow b_{3u}^*$	2.45	0.30	2.1			
			0.40				
RbCl	$a_{1g} \rightarrow b_{2u}$	1.71	0.11	1.0			
	$a_{1g} \rightarrow b_{3u}$	1.78	0.22	0.33			
	$a_{1g} \rightarrow b_{1u}$	1.93	0.24	2.3			
	$a_{1g} \rightarrow b_{3u}^*$	2.20	0.10	0.60			
			0.34				

<sup>a)</sup> K. S. Song, A. M. Stoneham and A. H. Harker: J. Phys. **C8**, 1125 (1975).

<sup>b)</sup> A. M. Stoneham: J. Phys. **C7**, 2476 (1974).

<sup>c)</sup> N. Itoh, A. M. Stoneham and A. H. Harker: J. Phys. **C10**, 4197 (1977).

<sup>d)</sup> F. Okamoto: Phys. Rev. **124**, 1090 (1961).

states and subsequently be de-excited to lower states. Alternatively if a self-trapped positive hole traps an electron, it will first occupy the highest orbital and de-excited successively to the lower states. Thus in order to understand the mechanisms of the photochemical processes and the detailed de-excitation processes, the location of the excited states at the relaxed configuration is essential.

The optical absorption of the self-trapped excitons perturbed by monovalent alkali impurities was also measured, for KCl:Na,<sup>22)</sup> and KBr:Na.<sup>23)</sup> It has been shown that the self-trapped excitons perturbed by monovalent alkali impurities exhibit nearly the same optical absorption spectra as unperturbed self-trapped excitons. The detailed dichroic spectroscopy was also measured for the self-trapped excitons in KCl perturbed by Na<sup>+</sup>. The energetic order of the state was found to be not modified by the association of a self-trapped exciton with a monovalent alkali impurity.

#### 4. 2. Higher excited states of rare gas solids

The excitons in the rare gas solids are rather similar to those in alkali halides in the sense that they consist of a hole in p-type orbital and an electron. It is known that the excitons in Ne, Ar and Kr are self-trapped. The optical absorption spectra of the self-trapped excitons in Ne, Ar, and Kr crystals have been measured by Suemoto and Kanzaki.<sup>24, 25)</sup> They observed an atomic-type self-

trapped excitons, as well as the molecular-type self-trapped excitons the latter being similar to those in alkali halides in these crystals. The atomic type self-trapped excitons have a lifetime different from that of the molecular-type self-trapped excitons and its transition energies are very similar to those of Ne gas. They also found that photoexcitation of one causes transformation to the other.<sup>26)</sup>

Further interesting result on the optical absorption of the self-trapped excitons in Ne is that the atomic type self-trapped exciton becomes a nucleus of the cavity or the vacancy cluster. The optical absorption of the atomic type self-trapped excitons obtained at several delay times after irradiation with an electron pulse is shown in Fig. 19. Clearly the peak position of the optical absorption band shifts as time after the pulse increases. Suemoto and Kanzaki have shown that the shift of the peak position saturates and that the final peak position as well as the initial peak position does not depend on temperature. However the speed of the shift has been found to be faster at higher temperatures. The shift has been ascribed to the thermal coagulation of vacancies around an excited Ne atom in a Ne crystal.

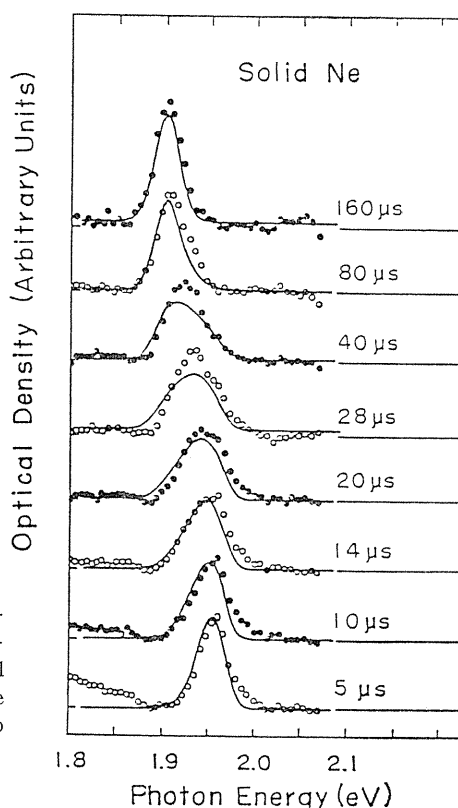


Fig. 19. Time-resolved optical absorption spectra of the atomic type self-trapped excitons in solid Ne. The shift of the optical absorption peak has been ascribed to the association with vacancies (after Suemoto and Kanzaki<sup>25)</sup>).

#### 4. 3. Higher excited states of triplet excitons in molecular crystals

The T-T absorption of various molecules has been studied extensively. It is interesting to see whether there is a solid state effect on the T-T absorption. In solids the triplet state is in a form of the plane wave and may be also influenced by the superlattice structures. Thus two types of solid state effects are dealt with in this paper: the effect of the translational symmetry in a naphthalene crystal and the effect of the presence of the superlattice in a dibromonaphthalene crystal.

The optical absorption due to the triplet excitons in naphthalene has been

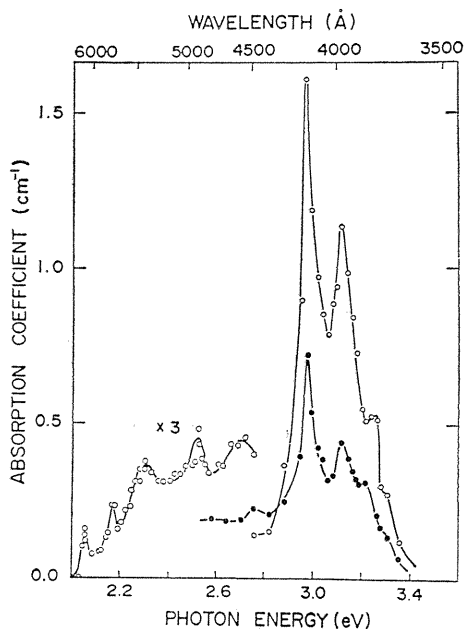


Fig. 20. Wavelength dependence of the transient optical absorption induced by an electron pulse in a naphthalene crystal, measured with a-polarized (open circles) and b-polarized (closed circles) light at 298K (Higuchi et al.<sup>27</sup>). The highest peak is due to the  ${}^3B_{1g}^- \leftarrow {}^3B_{2u}^+$  transition.

studied by Higuchi et al.<sup>27</sup>) They observed the optical absorption bands that are rather similar to those of naphthalene molecules as shown in Fig. 20. They showed, however, that the width of the optical absorption band from the lowest  ${}^3B_{2u}^+$  exciton to the  ${}^3B_{1g}^-$  exciton is larger than the width of the same transition line in a molecule. They suggested that the width of the absorption band arises from the width of the upper exciton band. Since the width of the lowest triplet exciton is only 1 meV, the distribution of excitons in the lowest band at room temperature is practically uniform. Thus they concluded that the shape of the optical absorption band represents the density of states of the upper exciton band. They also studied the optical absorption at lower temperatures and showed that the observed polarization is in accordance with the expectation that the optical absorption is a band-to-band transition.

The effect of the superlattice structure has been observed in dibromonaphthalene. The unit cell of the dibromonaphthalene consists of 8 molecules belonging to 4 asymmetric units. Thus the triplet states in the crystal have asymmetry splitting beside the Davydov splitting. The T-T absorption in a crystal and in a solution of dibromonaphthalene was compared by Kojima et al.<sup>28</sup>) They found that the T-T absorption band in a crystal is wider than that in a solution and that the former can be described in terms of superposition of two absorption bands with the same shape as that obtained in a solution and with a separation of 97 meV, which was ascribed to the asymmetry splitting in the  ${}^3B_{1g}$  exciton in dibromonaphthalene.

As seen from a few examples, the studies of the so-called T-T absorption in solids is very useful to make clear the electronic nature of the higher excited states. These studies are of basic importance for studies of de-excitation and photochemical processes being discussed in next paragraph.

Here we note the difference in the absorption spectrum obtained at the ground state and that obtained from the (relaxed) excited state. The initial state of the optical absorption in the latter case is in the relaxed configuration. Therefore because of the Frank-Condon principle, which states that the optical transition in the configurational coordinate diagram is vertical, the optical absorption spectroscopy from the lowest exciton state enables us to survey the higher electronic state at the relaxed configuration. Particularly when the ground state has a high symmetry, this is an advantage, since the excitation can be made to each of symmetry-split states.

#### V. Studies of the photochemical reaction and the other non-radiative processes at highly excited states

One of the current interest on the photochemical reaction in general is to identify the initial state from which the reaction products are evolved. From the discussion at the end of the last section, it is clear that the excitation spectroscopy of a photochemical reaction in alkali halides at the relaxed configuration, or the double excitation spectroscopy, enables us to obtain the yield of the photochemical process at each of the symmetry-split states. Studies of the excitation spectroscopy at the unrelaxed configuration gives only the reaction yield at the degenerate state. This is not sufficient to make clear the reaction mechanism. In this section we deal with the excitation spectroscopy at the relaxed configuration.

##### 5. 1. Kinetics of de-excitation and reactions at the excited states

In this section we discuss the information which we can derive out of the studies of the double excitation spectroscopy for the creation of a Frenkel pair from a self-trapped exciton. In these experiments the self-trapped excitons at the lowest triplet state were generated with an electron pulse and they were excited with a light pulse that are delayed from the electron pulse within the lifetime of the self-trapped exciton.<sup>29~31)</sup> Measurements have been made of the self-trapped excitons annihilated by the laser excitation and of the Fcenters or the Hcenters created. To study the double-excitation spectrum for the intersystem crossing, the creation of the singlet luminescence as well as the reduction of the triplet luminescence was also measured.

The number  $\Delta N_T$  of the lowest triplet self-trapped excitons annihilated by the laser irradiation was determined either by measurements of the change  $\Delta\alpha_T$  in the optical absorption coefficient or of the change  $\Delta I_T$  in the intensity of the  $\pi$ -luminescence. The concentration  $\Delta N_F$  of *F* centers and that  $\Delta N_H$  of the *H* centers were determined by measurements of the change  $\Delta\alpha_F$  and  $\Delta\alpha_H$  of the optical absorption coefficients at the maximum of the respective optical absorption bands. The concentration  $\Delta N_S$  of the generated singlet luminescent states was determined from the measurements of the increment  $\Delta I_S$  of the singlet luminescence. Typical oscilloscope trace for the intersystem crossing and the reaction measurements are shown in Fig. 21. The concentration changes  $\Delta N_S$  and  $\Delta N_T$  were obtained by using following equations:

$$\Delta N_S = G\tau_S \Delta I_S \quad (8)$$

$$\Delta N_T = G\tau_T \Delta I_T, \quad (9)$$

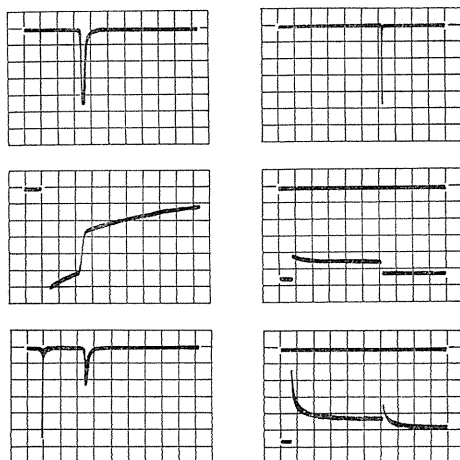


Fig. 21. Typical oscilloscope traces of the double excitation spectroscopy. The upper figures in the left and right hand sides show the incidence of the light pulse. The left-hand side shows the change in the  $\sigma$ - and  $\pi$ -luminescence and the right-hand side shows the optical absorption due to the  $F$  centers and the lowest triplet selftrapped excitons.

where  $G$  is the geometrical factor, and  $\tau_s$  and  $\tau_T$  are the lifetimes of the  $\sigma$ - and  $\pi$ -luminescent states, or by using the Smakula's equation:

$$\Delta N_f f_f = \frac{9mc}{\pi e^2 \hbar} \frac{n}{(n^2 + 2)^2} \Delta \alpha_f W_f \quad (10)$$

$$\Delta N_{II} f_{II} = \frac{9mc}{\pi e^2 \hbar} \frac{n}{(n^2 + 2)^2} \Delta \alpha_{II} W_{II} \quad (11)$$

$$\Delta N_r f_r = \frac{9mc}{\pi e^2 \hbar} \frac{n}{(n^2 + 2)^2} \Delta \alpha_r W_r, \quad (12)$$

where  $f$ 's are the oscillator strengths,  $W$ 's are the half-widths of the optical absorption band,  $n$  is the refractive index and  $m$  is the electron mass.

A theoretical treatment of the de-excitation kinetics indicates that<sup>30)</sup>

$$\frac{\Delta N_r}{N_r} = 1 - \exp\left[-\frac{\eta_s}{\eta_s + \eta_F + \eta_X} \sigma \phi t\right], \quad (13)$$

$$\frac{\Delta N_s}{N_r} = \frac{\eta_s}{\eta_s + \eta_F + \eta_X} \left(1 - \exp\left[-\frac{\eta_s}{\eta_s + \eta_F + \eta_X} \sigma \phi t\right]\right), \quad (14)$$

and

$$\frac{\Delta N_s}{N_r} = \frac{\eta_F}{\eta_s + \eta_F + \eta_X} \left(1 - \exp\left[-\frac{\eta_F}{\eta_s + \eta_F + \eta_X} \sigma \phi t\right]\right), \quad (15)$$

where  $\eta$ 's are the quantum yields of the transition to the state, specified by the suffix, from the excited state populated by excitation with laser light. The suffix  $S$  and  $F$  denote the  $\sigma$ -luminescent state and  $F$ - $H$  pair, while  $X$  denotes the state other than these two states and the lowest triplet state of the self-trapped excitons. The quantum yield  $\eta$ 's are those of creating the singlet luminescent state,

the  $F$ - $H$  pair and the  $X$  state upon excitation to a given excited state. When the lowest triplet exciton is excited to a certain higher state, the de-excitation occurs through vibronic states associated with several electronic states lying between the state to which excitation is made and the lowest triplet states. Thus if the transition rate to the next lower state is much higher than that to the other states, the quantum yield  $\eta_s$  is, for instance, the summation of the quantum yield  $\eta_s^i$  of reaching the singlet luminescent state from vibronic states  $i$  lying between the initial state and the lowest state:

$$\eta_s = \sum_i \eta_s^i. \quad (16)$$

Comparison of Eqs (13), (14) and (15) yields

$$R_s = \frac{\Delta N_s}{\Delta N_T} = \frac{\eta_s}{\eta_s + \eta_F + \eta_X}, \quad (17)$$

and

$$R_F = \frac{\Delta N_F}{\Delta N_T} = \frac{\eta_F}{\eta_s + \eta_F + \eta_X}. \quad (18)$$

$R_s$  and  $R_F$  are the branching ratios of creating the singlet luminescent state and the  $F$  centers upon excitation of the lowest triplet exciton to a given excited state.

### 5. 2. $F$ - $H$ -pair creation and intersystem crossing in NaCl and KCl

The creation of the  $F$ - $H$  pairs at excited states of the self-trapped excitons by means of the double excitation spectroscopy has been studied by Soda *et al.*<sup>30,31)</sup> The same authors have also measured the intersystem crossing at excited states of the self-trapped excitons.<sup>29, 31)</sup> In this section we describe their experimental results briefly and discuss on the information derived out of these experimental studies.

The typical experimental results for  $R_s$  and  $R_F$  as a function of photon energy for KCl and NaCl are shown in Figs. 22 and 23. Evidently the creation of the  $F$  centers takes place by excitation to the next lowest state of the self-trapped excitons reached through an allowed optical transition in KCl and NaCl. In KCl,  $R_F$  is practically independent of the photon energy of the laser light. This result was taken as an indication that the internal conversion after the excitation to the higher states leads to the next lowest state of the self-trapped excitons, without any additional creation of  $F$  centers directly from the higher excited states. Thus it has been concluded that one of the states  $A_{1g}(b_{3u}; b_{3u})$  or  $B_{1g}(b_{2u}; b_{3u})$  state\* is the origin of the  $F$ - $H$  pair. Most probably the  $F$ - $H$  pairs will be evolved from one of these states and the initial state of the  $\sigma$ -luminescence will be evolved from the other.

In NaCl, the similar conclusion described above may be derived but in this case when the excitation is made to the higher  $A_{1g}^*(b_{3u}^*; b_{3u})$  state, no  $F$ - $H$ -pair creation takes place. Clearly the de-excitation from the higher state bypass the state that causes the  $F$ - $H$  creation. Such bypassing of the states during de-

---

\* The capital letter indicates the irreducible representation of the state and the small letter before semicolon indicates the electron orbital and that after the semicolon the hole orbital.

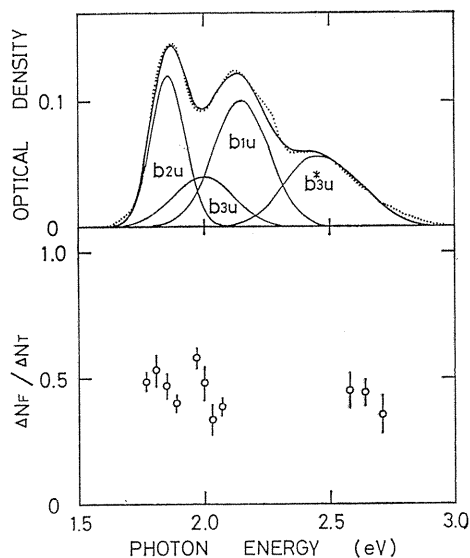


Fig. 22. The dependence of the creation yield of the  $F$  centers in KCl from the excited states of the self-trapped excitons on energy of photons bombarded in order to excite the lowest triplet self-trapped excitons. Upper part of the figure shows the optical absorption spectra (see Fig. 18, after Soda and Itoh<sup>30</sup>).

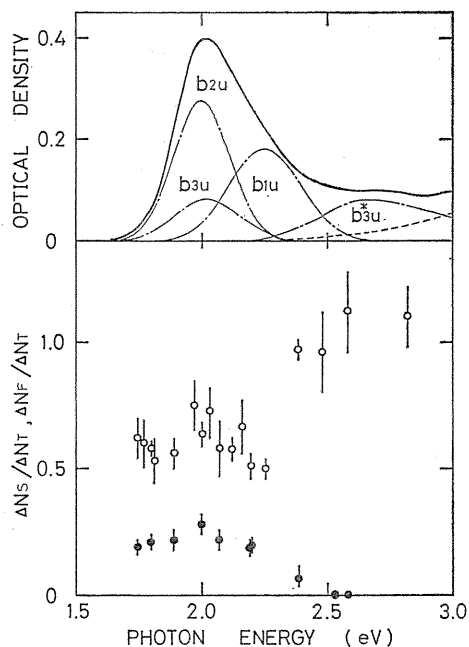


Fig. 23. The dependence of the creation yield of the  $F$  centers (closed circles) and the  $\sigma$ -luminescence (open circles) in NaCl from the excited states of the self-trapped excitons on energy of photons bombarded in order to excite the lowest triplet self-trapped excitons. Upper part of the figure shows the optical absorption spectra of the self-trapped excitons in NaCl (after Soda and Itoh<sup>31</sup>).

excitation may be understood in terms of strong electron-lattice coupling. These phenomena are of importance to understand the non-radiative processes as well as photochemical processes in solids.

Another important consequence of the investigation of the double excitation spectroscopic technique is the observation that the yield of the  $F$ - $H$  creation as well as the intersystem crossing is usually not more than 10%.<sup>31</sup> Thus the predominant channel of the non-radiative de-excitation is the internal conversion within the triplet manifold. Moreover it has been found that the delay in the build-up of the lowest triplet state is only about 100ps.<sup>32, 33</sup> These results are not surprising since electronic states are densely populated above the  $A_{1g}$  and  $B_{1g}$  states. The next low-lying state from the  $A_{1g}$  state is rather separated, but the strong electron-lattice coupling again may cause the very rapid non-radiative transition from the  $A_{1g}$  or  $B_{1g}$  state to the lowest state of the triplet exciton.

Even though the original state of the  $F$ - $H$  pair creation has not been determined, a new technique is being developed to identify the original state. The



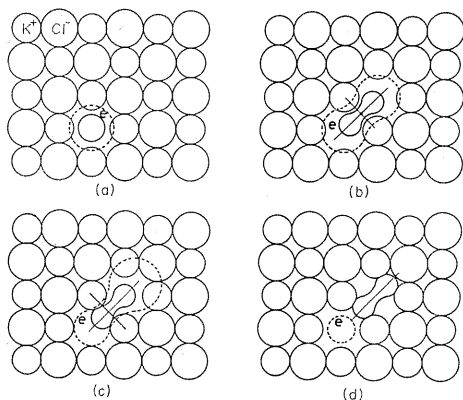


Fig. 24. A schematic diagram indicating the self-trapping of an exciton and the evolution of a Frenkel pair from a self-trapped exciton.

technique is essentially based on the anisotropic nature of the self-trapped exciton and is utilizing the dichroic excitation. To identify the state has an important implication on the mechanisms of defect creation from the electronically excited states. Toyozawa<sup>34)</sup> has suggested the adiabatic instability at the relaxed configuration for the motion of the  $\text{Cl}_2^-$  molecular ion along a  $\langle 110 \rangle$  direction (see Fig. 24). This adiabatic instability is induced at the  $A_{1g}$  ( $b_{3u}; b_{3u}$ ) state by an accidental Jahn-Teller effect between the  $b_{3u}$  orbital and the lowest  $a_{1g}$  orbital. On the other hand, Itoh and Saidoh<sup>35)</sup> have suggested that the weakening the repulsive potential between the halogen molecular ion and two alkali ions lying on the direction perpendicular to the molecular ion is essential. The repulsive potential is shown<sup>36, 37)</sup> to be weakened if the positive hole in the halogen molecular ion is excited.

### 5. 3. Detrapping of impurity-trapped excitons by photo-excitation

The thermal detrapping of free excitons from defects or impurities has been studied extensively. Using the experimental technique of the double excitation, the optical detrapping of excitons in a naphthalene single crystal, trapped by chloronaphthalene, has been studied by Shirakawa *et al.*<sup>38)</sup> They measured the fluorescence induced by collisions of a detrapped exciton with a trapped exciton. From the experimental results they derived the detrapping probability as a function of photon energy, which is shown in Fig. 25.

Similarly to the case of the photon energy dependence of the  $F$ -center creation, the first derivative of the yield curve means the detrapping probability from the state to which excitons are excited. The results shown in Fig. 25 indicate that the

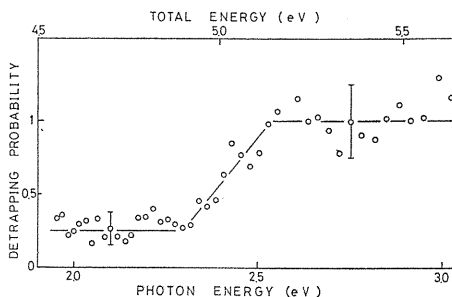


Fig. 25. The optical detrapping probability of an exciton in a naphthalene crystal trapped by a chloronaphthalene impurity, as a function of photon energy at 4.2 K (after Shirakawa *et al.*<sup>38)</sup>).

first derivative is non-zero between 2.3 and 2.5 eV and at some energies below 2.0 eV. In the other states highly excited excitons are de-excited through collisions with phonons, namely through the internal conversion. The non-zero detrapping yield between 2.3 eV and 2.5 eV has been ascribed to the admixture between the exciton state and the free electron-hole state, from the energetic arguments. The location of the lower state has not been made but it will be related to the free triplet exciton state. If so it will be very small since the depth of the trapped state against the free triplet exciton is only 30 meV.<sup>39)</sup>

## VI. Dynamics of defects induced by ionizing irradiation in alkali halides

Electron pulses can be utilized for studies of defect dynamics. Here by defect dynamics we refer to the motion, aggregation, impurity trapping and annealing of defects. Following methods may be utilized: (1) The direct determination of electron-pulse-induced defect creation and defect annealing and (2) Comparison of the defects formed in pure and doped crystals within a pulsed bombardment. The former technique enables us to observe the defect motion taking place with a delay longer than the duration of the pulse. The latter technique makes it feasible to derive information on the defect motion terminated during the electron pulse. This technique can distinguish the effect of the defect motion in the process of formation from the that of the thermal motion.

### 6. 1. Defect dynamics in the defect creation processes

When an  $F$ - $H$  pair is created by a photochemical process, a certain amount of energy is imparted to the interstitial. Thus the  $H$  center created is usually separated from the  $F$  center position from which the  $H$  center is originated. The motion of the interstitial until it is de-energized has been called the dynamic motion and is distinguished from the thermal motion.<sup>40)</sup> Figure 26 shows a typical experimental result which distinguishes the dynamic motion from the thermal motion.<sup>41)</sup> The result indicates the number of the  $H$  centers, the  $F$  centers and the di- $H$  centers created by an electron pulse, as a function of time after the pulse. Immediately after an electron pulse one sees that both the  $H$  centers and the di- $H$  centers are created. There is slow decrease of the  $H$  center concentration, which is compensated by creation of the di- $H$  centers. The extrapolation of the growth curve does not lead to zero. Moreover, the temperature dependence of the slowly increasing component was found to agree with that of the thermal motion. On the other hand the number of the di- $H$  centers formed immediately after an electron pulse depends on temperature following an Arrhenius equation but with a different activation energy.<sup>40)</sup>

The experimental results described above can distinguish the motion during bombardment and after bombardment. The motion during bombardment may be either ascribed to the dynamic motion, described above, or the radiation-enhanced diffusion of the  $H$  centers. The enhanced diffusion of the  $H$  centers will become less effective as the lifetime of the  $H$  centers becomes less than the electron-pulse duration. In alkali halides it has been found that the creation of the di- $H$  centers during the electron pulse takes place even at high temperatures,<sup>41)</sup> where the lifetime

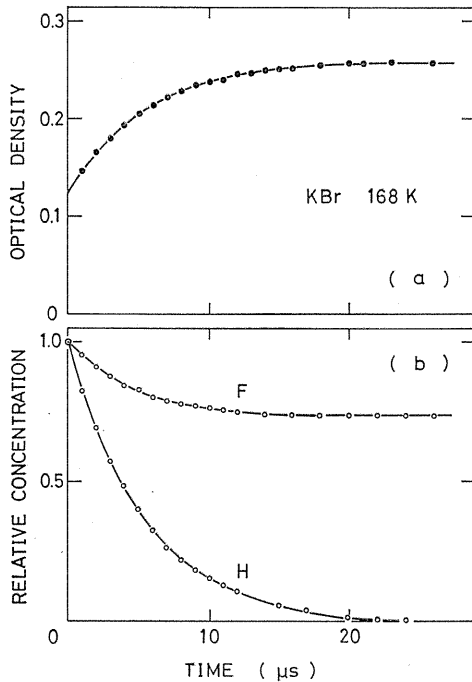


Fig. 26. Annihilation of the  $F$  centers and the  $H$  centers (lower) and the formation of the di- $H$  centers (upper) after an electron-pulse bombardment in KBr at 168K (after Tanimura and Itoh<sup>41</sup>).

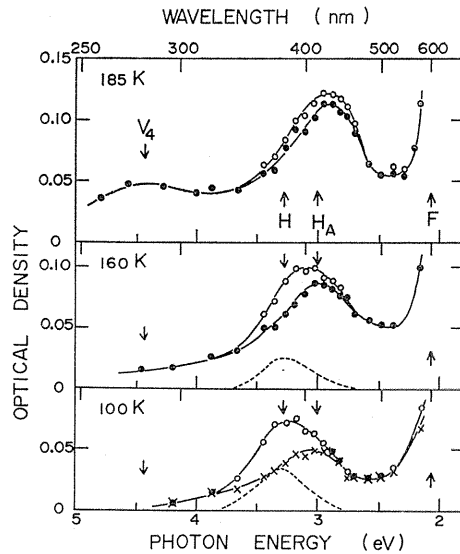


Fig. 27. Optical absorption bands formed by an electron-pulse bombardment in KBr: Na. The apparent peak shift with increasing temperature is due to the increasing formation yield of the  $H_A$  center (the peak of the  $H_A$  band is at 3.26 eV, after Saidoh *et al.*<sup>40</sup>).

of the  $H$  centers is expected to be very small.<sup>35)</sup>

The dynamic motion has been studied in detail by Saidoh and coworkers.<sup>42~44)</sup> These authors measured the interaction between two  $H$  centers and between an  $H$  center and a monovalent impurity in alkali halides between 100K and 200K. A typical result for the interaction between the  $H$  center and the  $Na^+$  impurity is shown in Fig. 27. Clearly the increase in temperature enhances the creation yield of the  $H_A$  center, the  $H$  center trapped by  $Na^+$  impurity. They analyzed the results such as shown in Fig. 27 with an assumption that the interaction takes place while the interstitials undergo a dynamic motion. They showed that the range  $l$  of the dynamic motion depends on temperature as

$$l = l_0 + l_1 e^{-E/kT}, \quad (19)$$

where  $l_0$  and  $l_1$  are constants.  $l_0$  is typically a few lattice distances. These quantities are related to the sputtering and other associated processes.<sup>45)</sup>

There are other few advantages in employing electron pulses to study the defect interaction. One important advantage is that one measures defects created in a short pulse in which neither thermal motion of interstitials nor thermal decomposition of defect is allowed. This fact often simplifies the analysis. For example, the

concentration relation between defects, such as a quadratic relation, often helps to identify the defects. For example the di- $H$  center concentration formed under a quasi-steady state is proportional to the square of the  $H$ -center concentration. Hoshi et al.<sup>43)</sup> have used an electron pulse to find that the  $D_3$  center is a di- $H$  center stabilized by a Ca impurity in alkali halides.

### 6. 2. Dynamics of the primary defects

Observation of the post-irradiation behaviors of the defects introduced by a nanosecond electron pulse is often useful to make clear the defect dynamics. An advantage of using nanosecond electron pulses over using continuous irradiation is following. Under continuous irradiation defects introduced at the beginning of irradiation are influenced under irradiation. Since the irradiation time is long, the phonon-assisted motion under irradiation, such as the radiation-enhanced diffusion may alter the defect states. On the other hand the nanosecond irradiation creates defects in such a way that is not influenced by a long time irradiation effect. Therefore the defects created by a nanosecond electron pulse are not necessarily the same as those created by continuous irradiation even though the radiation dose is the same. The creation of defects introduced by a nanosecond electron pulse is, in a sense, a simulation of those in a track of heavy charged particles.

In order to demonstrate the difference in the defects created by a nanosecond pulse and by continuous irradiation, we show in Fig. 28, the optical absorption spectra after two types of irradiation. For the electron pulse irradiation, spectrum was obtained 100ns after the electron pulse. The  $F$  band is identical but the uv bands are not the same. The band after the nanosecond irradiation, being referred to as  $H_s$  band, is a new band which has not been observed by continuous irradiation.<sup>47)</sup> The  $V_4$  band, which has been ascribed to the di- $H$  center, is known to be stable below 200K. The  $V_2$  band has been assigned to be the optical absorption of halogen molecules embedded in dislocation loops.<sup>48)</sup>

Annealing of the  $F$  centers created by a nanosecond electron pulse has been measured.<sup>48)</sup> Typical example is shown in Fig. 29. Comparison of these annealing curves with those of the  $V_4$  centers and the  $H_s$  centers shows that the first two stages, marked I and II, are caused by interstitial-vacancy annihilation. The annealing of the irradiation-induced volume expansion has been also measured,<sup>48)</sup> as shown in Fig. 30 and it has been found that the stages I and II are accompanied by the annealing of the volume expansion but in the later stages the annealing of the volume expansion does not necessarily follow the annealing of the  $F$  centers. Similar results have been obtained for NaCl.

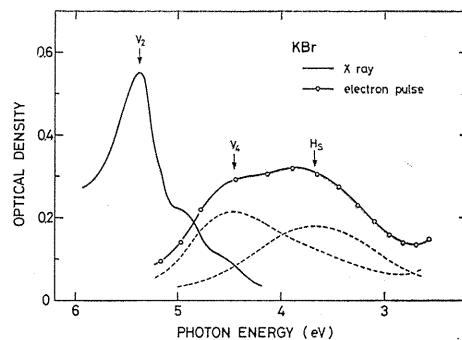


Fig. 28. Comparison of the optical absorption bands in the uv region, formed by an electron pulse and by continuous X-ray irradiation at room temperature in KBr.

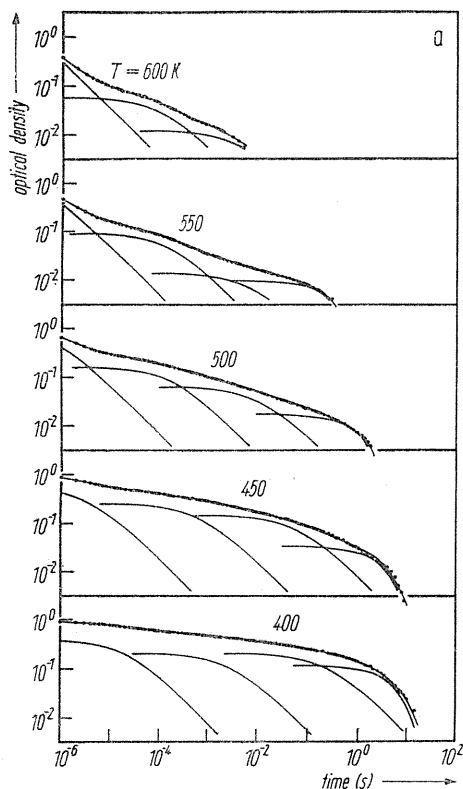


Fig. 29. A typical decay curve of the  $F$  centers in KBr formed by an electron pulse. The thin solid lines show the result of the decomposition into four annealing stages. Stages I, II and III are bimolecular and stage IV is monomolecular (after Toriumi and Itoh<sup>41</sup>).

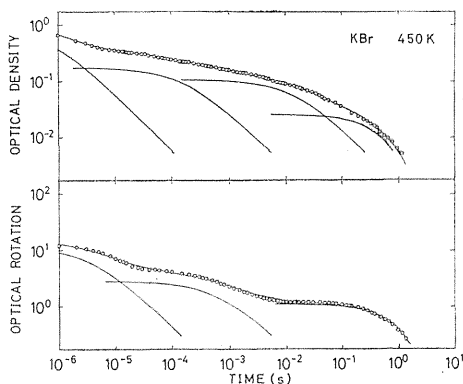


Fig. 30. Comparison of the annihilation of the  $F$  centers and the volume expansion after an electron-pulse bombardment in KBr. No stage III is observed in the volume expansion.

The results described above indicate very clearly that the stages I and II are due to the direct recombination of  $F$  centers with two types of the di- $H$  centers that are mobile at respective jump rate. In view of the experimental results that the  $F$ -centers in alkali halides make little contribution to the volume expansion, it has been suggested that the annealing stage of the  $F$  centers not accompanied by the volume change is due to the coagulation of the  $F$  centers into clusters. The annihilation of the  $F$  centers may induce the growth of the cluster size. This result explains the experimental results that the annealing at the last stage is a mono-molecular reaction.

It is interesting to note that if higher temperature annealing stages does not leave any defects, the radiation damages of materials will not take place. The reason why the radiation damage occurs at high temperatures is that vacancies and interstitials are clustered separately rather than annihilate each other. Thus it is essentially important to find the conditions at which the defect clustering is induced. The studies described above indicate that the  $F$  centers of which the inter-

stitial partners are stabilized are coagulated, while those of which interstitial partners are not stabilized are annihilated. Thus one important criterion for clusterization appears to be the formation of interstitial stabilization with an energy larger than the migration energy of vacancies.

### VII. Concluding remarks

The use of the Febetron 707 has yielded varieties of information which otherwise can not be obtained. Particularly the studies of the double-excitation spectroscopy, the exciton dynamics and defect kinetics will be of use to other systems. Following extension of the present techniques may facilitate further deep understanding on the non-radiative processes and defect dynamics.

(1) The use of picosecond dye-laser will be of particular importance. The delay time in the non-radiative de-excitation is of the order of a few picoseconds. Therefore if a picosecond laser is used instead of a nanosecond laser, the delay time in the build-up of the evacuated lowest triplet state can be determined. By changing the photon energy the non-radiative transition rate between each of the higher excited states can be obtained. The pathway of the non-radiative transition and the structure of vibronic states may be made clear. In the highly excited states, because of pseudo-Jahn-Teller effect, the electron-lattice coupling will produce the mixed electronic states and strongly influence the non-radiative pathways. The studies of the non-radiative processes using the double excitation technique may open a new field, non-radiative processes in a low symmetry, and is useful to understand photochemical processes.

(2) Use of high intensity electron pulse will be important. One of the current interest of radiation effects is the high density electronic excitation effect induced in a track of heavy ions that exhibit very high energy deposition rate. It is, however, often not very practical to study the high density effect using heavy ions, because of the difficulty in controlling the energy deposition rate and of the presence of the effect of elastic collisions. Use of the high intensity electron pulse for studies for example, of the high density effect on sputtering, chemical reactivities and luminescence will be useful. Focussing the Febetron beam by two orders of magnitude may suffice for this purpose.

(3) The studies of the type that have been made for alkali halides and aromatic hydrocarbon crystals can be extended into any materials. In science it is often the case that use of a new technique cause a stepwise progress. In this sense it is hoped that similar techniques may be used extensively by experts of other fields.

### References

- 1) L. M. Dorfman and M. S. Matheson, *Progress in Reaction Kinetics III*, ed. G. Porter (Pergamon, New York, 1965).
- 2) F. Seitz and J. S. Koehler, *Solid State Physics*, eds F. Seitz and D. Turnbull (Academic Press, New York, 1956).
- 3) K. Toyozawa, in *Proc. 4th Intern. Conf. Vacuum Ultraviolet Radiation Physics* (Vieweg-Pergamon, Braunschweig, 1974), p. 317.
- 4) N. Itoh, *J. Phys. (Paris)*, **37**, C7-27 (1976).

- 5) R. T. Williams, *Semiconductors and Insulator*, 3, 251 (1978).
- 6) M. N. Kabler, "Point Defects in Solids" ed. by J. H. Crawford and L. M. Slifkin, Vol. 1 p. 201 (Plenum Press, New York, 1972).
- 7) P. Avakian and R. E. Merrifield, *Molecular Crystals* 5, 37 (1968).
- 8) R. T. Williams and M. N. Kabler, *Phys. Rev.* B9, 1897 (1974).
- 9) D. A. Wiegand and R. Smoluchowski, *Phys. Rev.* 116, 1069 (1959).
- 10) N. E. Geacintov and C. E. Swenberg, *Organic Molecular Photophysics*, ed. J. B. Birks (Wiley, New York, 1973) Vol. 1, p. 489.
- 11) H. Haken and S. Nikitine (eds), *Excitons at High Density* (Springer, Berlin, 1975).
- 12) T. Nakayama, M. Higuchi, S. Fujiwara and N. Itoh, *J. Luminescence* 12/13, 253 (1976).
- 13) S. Fujiwara, T. Nakayama, and N. Itoh, *Phys. Status Solidi*, B78, 519 (1976).
- 14) T. Chong and N. Itoh, *Phys. Status Solidi*, B74, 281 (1975).
- 15) K. Tanimura and N. Itoh, *J. Phys. Chem. Solids*, 42, 901 (1981).
- 16) T. R. Waite, *Phys. Rev.* 107, 463 (1957).
- 17) T. Tashiro, S. Takeuchi, M. Saidoh and N. Itoh, *Phys. Status Solidi*, B92, 611 (1979).
- 18) W. B. Fowler, *Color Centers in Solids* (Pergamon, New York, 1968).
- 19) J. H. Schulman and W. D. Compton, "Color Centers in Solids" (Pergamon, 1962).
- 20) R. T. Williams, *Phys. Rev. Letters* 36, 529 (1976).
- 21) K. Soda, K. Tanimura, and N. Itoh, *J. Phys. Soc. Jpn.* 50, 2385 (1981).
- 22) Y. Hirano and N. Itoh, *Phys. Letters* 60A, 465 (1977).
- 23) K. Tanimura, *J. Phys. C11*, 3835 (1978).
- 24) T. Suemoto and H. Kanzaki, *J. Phys. Soc. Jpn.* 46, 1554 (1979).
- 25) T. Suemoto and H. Kanzaki, *J. Phys. Soc. Jpn.* 49, 1039 (1980).
- 26) T. Suemoto and J. Kanzaki, *J. Phys. Soc. Jpn.*, in press.
- 27) M. Higuchi, T. Nakayama and N. Itoh *J. Phys. Soc. Jpn.* 40, 250 (1976).
- 28) K. Kojima, unpublished.
- 29) K. Soda and N. Itoh, *Phys. Letters* 73A, 45 (1979).
- 30) K. Soda and N. Itoh, *J. Phys. Soc. Jpn.* 48, 1618 (1980).
- 31) K. Soda and N. Itoh, *J. Phys. Soc. Jpn.* 50, 3988 (1981).
- 32) R. T. Williams, J. N. Bradford and W. L. Faust, *Phys. Rev.* B18, 7038 (1978).
- 33) Y. Suzuki, M. Okumura and M. Hirai, *J. Phys. Soc. Jpn.* 47, 184 (1979).
- 34) Y. Toyozawa, *J. Phys. Soc. Jpn.* 44, 482 (1978).
- 35) N. Itoh and M. Saidoh, *J. Phys. (Paris)*, C34-9, 101 (1973).
- 36) N. Itoh, A. M. Stoneham and A. H. Harker, *J. Phys. C10*, 4197 (1977).
- 37) N. Itoh, A. M. Stoneham and A. H. Harker, *J. Phys. Soc. Jpn.* 49, 1364 (1980).
- 38) A. Shirakawa, H. Asami, T. Nakayama, T. Chong and N. Itoh, *Solid State Commun.* 8, 625 (1978).
- 39) H. C. Wolf and H. Port, *J. Luminescence* 12/13, 33 (1976).
- 40) M. Saidoh, J. Hoshi and N. Itoh, *Solid State Commun.* 13, 431 (1973).
- 41) K. Tanimura and N. Itoh, *Radiation Effect Letters* 57, 155 (1980).
- 42) K. Toriumi and N. Itoh, *Phys. Status Solidi (b)* 107, 375 (1981).
- 43) M. Saidoh and N. Itoh, *J. Phys. Soc. Jpn.* 29, 156 (1970).
- 44) M. Saidoh and N. Itoh, *Phys. Status Solidi*, B72, 709 (1975).
- 45) M. Saidoh, J. Hoshi and N. Itoh, *J. Phys. Soc. Jpn.* 39, 155 (1975).
- 46) N. Itoh, *Nucl. Inst. and Methods*, 132, 201 (1976).
- 47) R. D. Saxena, K. Soda and N. Itoh, *Crys. Lattice Defects*, 8, 155 (1979).
- 48) L. W. Hobbs, A. E. Hughes and D. Pooley, *Proc. Roy. Soc. London A* 332, 167 (1973).
- 49) A. Koyano, unpublished (1981).